Microwave Single Photon Detection using Superconducting Circuits

A Thesis

submitted to

Indian Institute of Science Education and Research Pune

in partial fulfillment of the requirements for the

BS-MS Dual Degree Programme

by

Aniruddha Deshpande

Indian Institute of Science Education and Research Pune

Dr. Homi Bhabha Road,

Pashan, Pune 411008, INDIA.

April, 2020

Supervisor: Dr. R Vijayaraghavan

Certificate

This is to certify that this dissertation entitled *Microwave Single Photon Detection using Superconducting Circuits* towards the partial fulfilment of the BS-MS dual degree programme at the Indian Institute of Science Education and Research, Pune represents study/work carried out by Aniruddha Deshpande at Tata Institute of Fundamental Research, Mumbai under the supervision of Dr. R Vijayaraghavan, Professor, Department of Physics, TIFR, Mumbai, during the academic year 2019-2020.

Dr. R Vijayaraghavan

Aniruddha Deshpande

Committee:

Dr. R Vijayaraghavan

Dr. T S Mahesh

This thesis is dedicated my parents without whom this journey would not have been possible

Declaration

I hereby declare that the matter embodied in the report entitled *Microwave Single Photon Detection using Superconducting Circuits*, is the result of the work carried out by me at the Department of Physics, TIFR, Mumbai, under the supervision of Dr. R Vijayaraghavan and the same has not been submitted elsewhere for any other degree.

Dr. R Vijayaraghavan

Aniruddha Deshpande

Acknowledgment

I would first like to thank my supervisor Dr. Rajamani Vijayaraghavan for his constant guidance throughout this project. He has taught me an enormous amount, on variety of topics and gave me an insight of how real research works. I learned what it's like to be a scientist from him and what it's like to work in a research lab. Most of all I thank him for being so understanding and supporting despite all my blunders. I also thank him for maintaining a warm and amicable environment in the lab which made it a pleasure to work there. I would also like to thank my labmates Kishore, Anirban, Sumeru, Gaurav for the constant support throughtout the thesis.

I would also like to thank my past advisors and mentors who helped me throughout my coursework in IISER. I would like to thank my mentor and expert on MS thesis Dr. T S Mahesh for all the support he has shown in the previous years. His introductory course in Quantum Information is what inspired me in pursuing this specific field. I would also like to thank Dr. Seema Sharma for giving me key insights in experimental physics which turned out to be useful during my thesis.

My completion of this project could not have been completed without the constant support of my friends Ashwin, Atharva, Chinmay, Chandan, Kush, Jaideep, Prateek, Radhika, Rahul, Saswata, Madhav, Tushar, Prashant & Vishnu.

I would also like to thank IISER Pune for this wonderful journey and giving the opportunity to study at one of the best institutes in India. I also thank TIFR for allowing me to conduct my Master's thesis project. I also thank INSPIRE for financial support throughout my five years of study.

Finally I would like to thank my family for the unending love and enthusiasm for my work. I love you all and I dedicate my thesis to all of you.

x

Abstract

The field of quantum optics at microwave frequencies using superconducting circuits has progressed tremendously in the last 10 years. The availability of a non-dissipative, non-linear element like the Josephson junction combined with the ability to lithographically define structures for microwave propagation has pushed this field into new regimes previously impossible with optical light. The detection at optical frequencies is typically done using a photon detectors whereas the natural detector at microwave frequencies are linear amplifiers. Since the type of detection has a direct impact on the quantum state being observed, it is important to choose the right kind of detection technique for the particular application. Due to the low energy of the microwave photon, it makes it challenging to detect it. In this project, we reviewed the available technologies for single photon detection and studied different types of microwave photon detection protocols based on their pros and cons. We than tried to design single qubit and four qubit architecture after simulating the respective systems on COMSOL and Microwave Office.. We also performed two-tone spectroscopy to measure qubit's resonant frequency and anharmonicity. We futher measured relaxation times and dephasing times and found them to be very low than expected.

Contents

List of Figures

Chapter 1

Introduction

All computers, starting from Babbage's concept of programmable computers to the novel high performing supercomputers, follow the same principles. It consists of bits 0 & 1 and programs which are a set of logical operations. Classical computers are multi-purpose and have proved to be of immense help on a large scale. Although the speed of computation has improved tremendously over the past couple of decades, there are still problems unsolvable by classical computers. The aim of quantum computers is to tackle such problems by using the postulates of quantum mechanics.

The realization of Quantum computers can be accomplished by a variety of techniques including Trapped Ion, NMR, NV Centres, Superconducting Qubits, Quantum Dots, etc. Superconducting qubits are 2 level quantum systems consisting of superconducting electrical circuits, using Josephson junctions as nonlinear inductors and acting as artificial atoms. Based on Josephson energy E_j and Coulomb charging energy, for different cases, different types of qubits can be formed. Although three types of qubits exists(charge, flux and phase qubits) variety of other hybridizations also exist such as Transmon, Fluxonium, Quantronium, etc.

Single optical photon detectors absorbs the incoming photon, and use photon's energy as a measure to detect photon. This proves to be a real challenge in microwave photon detectors as the energy of single microwave photon is 5 orders of magnitude less than an optical photon. The goal of this thesis was to build a microwave single photon detector by first, studying the existing approaches and their drawbacks, and second, try to come up with a novel approach. Chapter 1 will serve as an introduction to cover the basics of superconducting circuits and circuit QED. Types of qubit, qubit readout and experimental techniques will be discussed here. Chapter 2 will discuss the essense of the thesis which is microwave photon detection.

Starting from single photon detection we will discuss clasifications of detection protocols and study the existing architectures. We will also look at the challenges faced by such detection schemes and try to study their solutions. In Chapter 3 we will look how the detector was modelled. It will include various qubit-cavity systems and their response by changing the parameters such as coupling & decay rate. We will study the qubit readout simulations to see how QND detection can help us. Chapter 4 contains what went into designing the detector. Different parameters to be measured, such as simulating the relaxation time(T1). It also contains simulating the physical design of the detector. Chapter 5 will discuss the results and measurements of the experiment. It contains the challenges faced while designing the detector and the drawbacks of our design.

Chapter 2

Superconducting Qubits and circuit QED

In classical computers, information is stored in bits where each bit can have a value of either '0' or '1'. This can be then used to process the information by running different algorithms. Quantum bits or 'qubits' differ slightly than classical bits. Qubits in addition to '0' and '1', has an additional state known as 'superposition' state or $a\,|0\rangle + b\,|1\rangle$ in which the qubit can coexist in both the states at the same time. However, when the qubit in superposition state is measured, the resulting state will either be '0' with probability $|a|^2$ or '1' with probability $|b|^2$, thus making the qubit collapse in either one of the states. These qubits form the building block for a Quantum computer. Such probabilistic behaviour of a system seems unfavourable to form a good basis for information processing. However as long as we keep avoiding measurement, the system will retain its 'quantum' nature.

Apart from the number of qubits, other factors such as decoherence time, ease of building qubit architecture, scalability, gate error rate are also taken into consideration while trying to build a fully-fledged quantum computer. To physically realize a quantum computer, different systems can be used based on their ability to form a 2 level system. Among them are, Superconducting qubits(superconducting circuits), NMR(nuclear spins), Trapped Ions, Quantum Dot(spin states of trapped electrons), BEC based quantum computer, Diamond based quantum computer(nuclear spins of Nitrogen vacancy centers in Diamond). We need to explore different architectures based on variety of We will be discussing the Superconducting qubits(circuits) in this thesis.

Superconducting qubit, a two-level quantum system, is a solid-state qubit, realized in a superconducting electrical circuit. In a superconductor, cooper pairs are the charge carriers,

unlike electrons in a regular conductor. The devices are typically designed in the radio frequency range and operate in the range of mK, using a dilution refrigerator. The key component used to build superconducting qubits is the Josephson junction. Josephson junction is the right candidate for the construction of superconducting qubits due to their long coherence times. In this chapter, we will study the theory of superconducting qubits and the methods used to study and control them.

2.0.1 Types of Qubits

The three primary qubit archetypes are phase, flux, and charge qubits. For qubit implementation, the logical quantum states must be mapped to the different states in the physical system. This is usually done on the qubit's discrete energy levels. In the case of a charge qubit, the number of cooper pairs on the superconductor is correlated with the discrete energy levels. For phase qubit, the distinct charge oscillation amplitudes across a Josephson junction are correlated with different energy levels. Finally, for flux qubit, the different energy levels are correspondent with an integer number of magnetic flux quanta in the superconducting device. The circuits of these qubits have one thing in common, Josephson junction. The junction consists of two or more superconductors, connected by a weak link. This link is an insulating material making it an S-I-S(Superconductor-Insulator-Superconductor) type junction. Quantum tunneling is responsible for the current to exist across a Josephson junction, which then is used to create nonlinear inductance. This helps in creating anharmonicity in the qubit design. Two energies are essential when designing a superconducting qubit. The Josephson energy, E_j, is a measure of the strength of the coupling across the junction, while the Coulomb charging energy, E_c, is the energy needed to increase the charge on the junction by 2e. The junction is essentially a capacitor with $E_c = \frac{4e^2}{2C}$, where e gives the charge of the electron and C gives the total capacitance.

The charge qubit is essentially a small superconductor, also called CPB(Cooper Pair Box). The CPB is driven with voltage Vg also known as gate voltage, via a capacitor and is connected to a Josephson junction(JJ). The states $|0\rangle$ & $|1\rangle$ (zero and one extra cooper pairs) have the same energy, given that for Cg capacitance of the gate, the gate voltage being $V_g = e/C_g$. A Flux qubit is made by connecting two JJs to form a closed superconducting loop. The qubit is controlled by varying the applied magnetic field and drive the circuit by adjusting the phase. The phase qubit encompasses a single junction, and the phase difference oscillations across the electrodes of the Josephson junction defines the two levels of the qubit. These different qubit archetypes can be differentiated based on the shape of their nonlinear

potential. The flux qubit has a quartic shape; phase qubit has cubic shape while the charge qubit has a cosine shaped potential. Apart from these three qubits, other modifications also exist, such as Transmon, Quantronium, Trimon, Xmon. Now that we have seen how the qubit is constructed, in the next section, we will study the hamiltonian and different limits for it.

2.0.2   Circuit QED

The method we use to couple the qubit system to the environment is called Circuit Quantum Electrodynamics or circuit QED. Circuit QED involves coupling a photon on a resonator chip to an artificial atom, unlike a natural atom in cavity QED. The first artificial atom was a Cooper-pair box or charge qubit. The number of cooper pairs on the superconducting island determines the state of the CPB qubit. The transition frequency of the qubit is adjusted by varying the coulomb energy and the Josephson energy. To make the CPB behave like a natural atom, the anharmonicity is necessary, which can be obtained due to the nonlinearity in the Josephson junction. Due to this anharmonicity, we can call it an artificial atom. The circuit QED architecture looks like a qubit placed inside a transmission line resonator that acts as a microwave cavity. The cavity QED system is characterized by the coupling strength g between the atomic transition and the electromagnetic field in the cavity, the rate (kappa) at which photons escape the cavity, and the rate (gamma) at which the atom decays into modes other than the cavity mode. In circuit QED, the coupling capacitance between the qubit and the resonator sets g, while the coupling capacitance between the resonator and the microwave environment sets (kappa).

The light-matter interaction here can be described by studying the Jaynes-Cummings Hamiltonian[16,17]. The circuit QED Hamiltonian contains the following terms; qubit term, cavity term, and the interaction term.

$$H = H_q + H_{cav} + H_{int}$$

The H_q term is a simple Zeeman term, H_{cav} term is cavity equivalent to quantum harmonic oscillator and the H_{int} (interaction term) signifies the coupling between qubit and the cavity, with coupling constant g. The full Hamiltonian is:

$$H = \frac{1}{2}\hbar\omega_q\hat{\sigma}_z + \hbar\omega_{cav}(\hat{a}^\dagger\hat{a} + \frac{1}{2}) + \hbar g(\hat{a} + \hat{a}^\dagger)(\hat{\sigma}_+ + \hat{\sigma}_-)$$

where $\hat{\sigma}_+$ & $\hat{\sigma}_-$ are raising and lowering operators operators for qubit given by $\frac{1}{2}(\hat{\sigma}_x \pm \hat{\sigma}_y)$ and a & $a^\dagger$ are annihilation and creation operators for cavity. If we expand the interaction term, we get four terms, but as we're in the limit where electromagnetic field frequency is close to the qubit transition, we can use Rotating wave approximation(RWA). We neglect the terms oscillating with high frequency i.e After making the rotating wave approximation, our Hamiltonian becomes:

$$H = \frac{1}{2}\hbar\omega_q\hat{\sigma}_z + \hbar\omega_{cav}(\hat{a}^\dagger\hat{a} + \frac{1}{2}) + \hbar g(\hat{a}\hat{\sigma}_+ + \hat{a}^\dagger\hat{\sigma}_-)$$

The interaction term couples the qubit and cavity states by allowing them to exchange quanta of energy. In the resonant limit, where $\omega_q = \omega_{cav}$, the degeneracy of the uncoupled spectra of the qubit and cavity is lifted by the presence of the coupling term in eigenstates of the system are then equal-weighted linear combinations of qubit and cavity. When ω_q and ω_{cav} are detuned from each other by an amount much more significant than the coupling g, the eigenstates of the JC Hamiltonian are approximately product states of qubit and cavity. This is known as the dispersive regime and is the subject of the next section.

2.0.3   Qubit Readout

Even though the interaction between qubit and cavity is ideal and lossless, we still need to measure the qubit state in the most efficient way possible. The main idea of the thesis includes a nondemolition photon detector, which will not disturb the incoming photon and still be able to read the qubit state. The interaction between qubit and cavity plays an essential role in this readout. We will introduce several photons in the cavity. These photons will act as our mediator for qubit state response. We will utilize the cavity's response to the qubit state change as our readout process. We will look at the methods we have tried using in the thesis i.e., Homodyne and Heterodyne detection and which one is more efficient. We will then look the standard dispersive readout used generally in all experiments.

In a heterodyne measurement, the frequency of the local oscillator is detuned from that of the signal. One can view this as rotating the measurement between the two quadrature amplitudes at a rate given by the detuning. Thus we obtain information about both quadratures. In Homodyne detection, which is a simplification of Heterodyne detection, the local oscillator frequency is equal to signal frequency, resulting in giving only one quadrature as a measurement output.

Now we'll look at the dispersive readout[16] which is used as measurement in many ex-

periements. This readout works because the cavity frequency and phase of the reflection coefficient for microwaves, depends on the state of the qubit. The phase of the microwaves reflected from the cavity is entangled with the state of the qubit and will consider the different back-action effects of measuring the phase of the microwaves or the photon number. The qubit is coupled to a detuned readout resonator, which can be imagined as a quantum harmonic oscillator, and the leaked field is amplified and used for QND measurement after the resonator is pumped. Depending on the resonator frequency, the resultant field will have a unique phase shift and amplitude, which then can be used to detect the state of the qubit (See Fig 2.1).
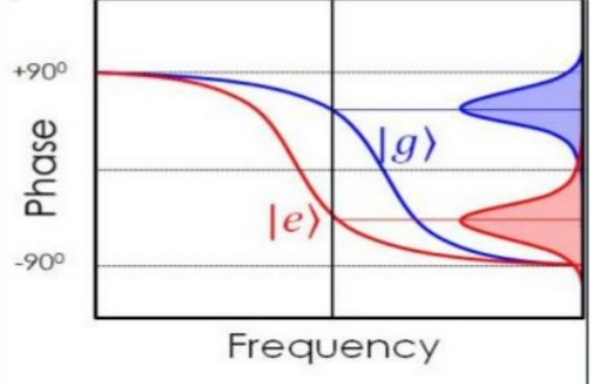

Figure 2.1: Qubit readout via dispersive shift: here phase shift (Adapted from ref. [17])

2.0.4 Experimental Techniques

This section highlights the different experimental techniques used in designing the circuits and carrying out the experiment. It will briefly cover the important components such as Cavity, Transmission line, Coplanar waveguide and will cover nano fabrication protocols such as e-beam lithography.

In the domain of circuit QED, cavity can be built using electrical circuits. The three main parameters in cavity are cavity frequency, Q-factor and impedance. For the energy state to have longer life time, high Q factor of cavity is necessarry. Size of the cavity controls the cavity frequency. The ratio of the width of center pin to the gap seperating center pin and ground plane determines the impedance. The coupling capacitors at input and output determine the value of quality factor. Some variations in cavity frequency are observed while changing the dimentions of coupling capacitors but such effects can be compensated. The resonant frequencies(mode dependent) of the cavity can be calculated by

$$\omega_c = \frac{c}{2\sqrt{\epsilon_r \mu_r}}\sqrt{(\frac{l}{x})^2 + (\frac{m}{y})^2 + (\frac{n}{z})^2}$$

9

where (x,y,z) are the dimentions of the rectangular cavity, (l,m,n) are mode numbers and c is the speed of light. The quality factor of the cavity depends on losses of two types; power loss in the walls and power loss in the dielectric filling the cavity.

We will now study the theory of microwave photon detection in brief. We will look at the classification and existing approaches microwave photo detection protocols. Their drawbacks and challenges will also be studied in detail.

Chapter 3

Microwave Photon Detection

Photons are defined as single quanta of energy or an initial excitation of a single mode of the quantized electromagnetic field. In 1905, along with the theory of quantas, Einstein also proposed the theory of a photon detector. In the past couple of decades, the research in photon detectors has made remarkable progress in developing detectors based on a variety of technologies such as photomultiplier tubes, quantum dots, superconducting qubits, and many others. In recent years, the field of quantum optics and quantum information has been interested in developing such detectors to work at the quantum limit or single-photon limit. Single-photon detectors are fundamental tools of research in quantum optics and play a pivotal role in the study of quantum information[11]. An ideal photon detector is expected to have a 100 % efficiency with no dark count. The research in building optical quantum computers, quantum cryptography, and quantum communication, require such high efficiency photon detectors to measure the signal accurately. As photons can travel long distances at the speed of light without interacting much with the environment, we observe low noise and low loss signals in the experiments. While using single-photon sources and detectors help many experiments in quantum optics experiments, several protocols such as quantum key distribution specifically have a prerequisite for single photons as more than one photon can jeopardize the security of the protocol allowing an eavesdropper to acquire information. Almost all photon detectors involve the conversion of the incoming photon into an electrical signal and measuring the electrical signal with high efficiency. We discuss here the existing approaches to microwave photon detectors. We will further discuss their benefits and drawbacks with respect to each other. We will also discuss how our qubit design is supposed to tackle the challenges these methods are facing.

Several optical single-photon detectors have been realized and have made developments in at-

taining near perfect detectors. Such devices allow complex analysis and manipulation of the radiation field, which is essential in the field of quantum information in the optical regime. However, microwave single-photon detectors have been challenging to implement, given that microwave photons have five orders of magnitude lower energy than optical photons. To attain such sensitive detectors variety of techniques are used, including circuit QED, single electron transistor[5, 10]. As the energy of the incoming photon is much less, the amount of noise should be very less resulting in low-temperature apparatus. Superconducting circuits operating in the range of mK prove to be of much use in this case. However, apart from detecting a photon with high efficiency, using circuit QED does not solve all the problems. There are several challenges in designing a photon detector at microwave regimes apart from attaining low temperatures. Current technology on cryogenic linear amplifiers is at a loss to resolve the single-photon regime.

Another challenge faced is the small cross-sections between microwave fields and qubits. Now, as qubit-qubit or qubit cavity couplings are necessary, cavities are used to amplify the coupling. This results in more problems, such as frequency mode matching. This results in a trade-off between the Q factor and reflectivity of the detector. Another significant disadvantage is the unfeasibility in measuring continuously without any backaction. This backaction imposes a limit on the efficiency of the detector. This is due to the Quantum Zeno effect[15]. This results in synchronizing the arrival of the measured field with the detection process. Due to the recent applications in hybrid optical microwave systems and microwave quantum systems, the demand for such detectors is high.

Now that we have laid the foundations for the concepts of a single-photon detector and it's applications, we will delve into the classification of photon detection based on techniques, robustness, and efficiency of the detector. The two main types of photon detection approaches are 1. Direct Detection, and 2. Indirect Detection. Direct detection includes absorbing the photon while detecting and measuring the count of the clicks[1]. This includes resetting the detector to the initial state after the photon is being detected. The incoming photon is lost in the process. In the case of Indirect photodetection, the incoming photon remains undisturbed, and the click is measured. This type of detection allows measurement in a continuous fashion along with photon arrival time[2].

The fundamental principle of Direct photon detection is the absorption of a quanta by the qubit in the ground state(naturally), which excites it to its excited at a higher level. This state change of the qubit is detected and verifies the presence of the photon

[1]. The most straightforward approach is an irreversible absorption of photons making the microwave photodetector a single shot. It is assumed that whenever photon enters the device, it is captured most of the time. If the qubit absorbs the photon, it's state changes to a more stable state, which is easier to observe. It implements a Λ-type three-level system with the incoming single photons having a frequency equal to one of the transitions in the system[1,6]. The excited state has a higher decay rate, thus it is unstable. When the photon interacts with the qubit in $|0\rangle$ (initial) state, the photon excites the qubit to $|1\rangle$ state and immediately decays to ground state $|g\rangle$ due to the high decay rate. This change in the state of the qubit ($|0\rangle$ to $|g\rangle$) is used for photon detection. The system has internal frequency ω and excited state to stable state decay rate Γ (**See Fig 3.1**).

The design involves a one-dimensional waveguide that is coupled to a set of photon absorbers placed randomly. As the probability of the qubit absorbing the photon is much less even at resonant frequency of the qubit, more than one qubit(absorber) is used. Once the photon interacts with the field, the qubit state changes. The final step consists of calculating the number of activated absorbers(qubit in a stable state), which is related to the number of photons. The efficiency of the detector varies by a different factor. Using only one qubit as an absorber, the detection efficiency has an upper limit of 50%. As we increase the number of qubits, it is possible to achieve near-perfect detection(**See Fig 3.2**). Another critical

Figure 3.1: Sketch of the one dimentional waveguide coupled to qubits placed arbitarily(above). Microwave field excites the qubit to unstable excited state which then decays into stable observable state(below) Adapted from ref. [1]

factor is the positioning of the absorber qubits along the waveguide. Placing the qubits close to each other results in them acting like a cluster of qubits or similar to single qubit with a high decay rate, which decreases the efficiency. Placing them longitudinally distant distinguishes each qubit apart and increases the efficiency. The maximum efficiency is seen to be increased from 50% for single qubit(N=1) to 95% for N=8[1]. Another research shows a near-perfect 100% efficiency is theoretically achievable with just one qubit as an absorber[4]. The idea of detection remains similar, but instead of an infinite waveguide, a semi-infinite
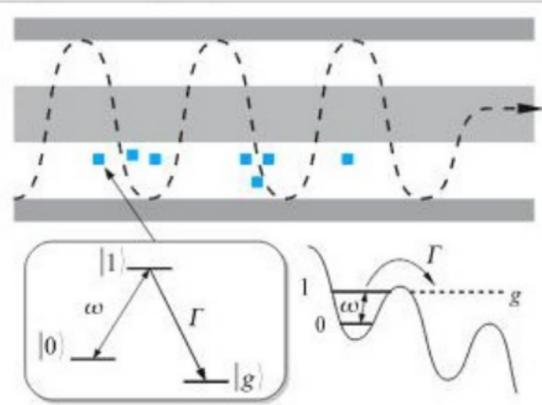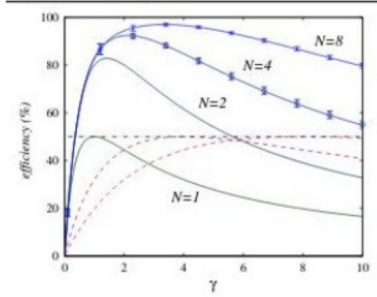
Figure 3.2: Detection efficiency varied with effective decay rate

Fig adapted from ref [1]

waveguide is used along with the three-level qubit system with the qubit placed at some distance from the end. This acts as a perfect mirror for the incoming photon[4].

The photon, if remained undetected the first time, will get another chance after bouncing back from the mirror and so on. This modification helps the detection process in achieving high efficiencies with a limited number of qubits. Although we can achieve high efficiency detectors with such methods, there certainly are some drawbacks which need to overcome. The exact qubit state readout is one of the major problems. The distinction of the state $|g\rangle$ might cause errors in detection efficiency. The fluctuations in the energies of the state $|0\rangle$ and $|1\rangle$, which changes the resonant frequency, also causes errors. This can be corrected by the bandwidth of the detector, which depends on the design. Another reason is the loss of photons after being absorbed due to the different non-radiative decay processes, which causes the $|1\rangle$ to $|0\rangle$ transitions. Leaky mirrors, photon losses can be ignored as the time scale of the photon wave packet is much smaller than those of these losses. Another major challenge is controlling the three level system to avoid dark counts or false positives. Such dark counts are caused by spontaneous transitions of the qubit from $|0\rangle$ state to $|g\rangle$ state. Resetting the detector to an initial $|0\rangle$ state periodically is also another way to get rid of this problem. Phase qubit can be used in such experiments, and the efficiency of this device is limited only by how it couples to the waves that contain the photons it has to detect. The limit of such detectors is that the detection is single-shot i.e., once the qubit absorbs a photon, it cannot absorb again unless its set to initial state[1,4]. This issue can be solved by another approach of photo detection namely Indirect Detection.

Indirect detection is the detection of incoming microwave photons without disturbing the photons. Such type of detection process is often called as Quantum Non Demolition(QND)

14

detection. The basic detection protocol proposes using an open waveguide where the microwave photon fields are coupled to the artificial atom via a strong nonlinear interaction[3, 14]. In such architectures, the system is coupled to a quantum probe such as homodyne or heterodyne signal. Such types of detection do not look directly for the microwave photon but analyses an observable which shifts in the presence of photons. Homodyne detection is a technique of measuring the information in the form of phase shift. This detection process is generally carried out in a dispersive regime via dispersive readout(Ch 1). A single microwave control photon causes a displacement in the probe field when present. The probe field is analyzed for the detection, the control field, however, is left unabsorbed. This makes the detection QND [2,8]. To experimentally realize such detection process, N three level transmons are coupled to the transmission line. The transmons are strongly anharmonic three level systems with resonant frequencies ω_{01} & ω_{12}. The incoming photon or control photon field is resonant with the qubit transition $|0\rangle$ - $|1\rangle$ while the probe field is resonant with $|2\rangle$ - $|1\rangle$. When the photon interacts with the system of qubits, it displaces the probe field[9]. This displacement is measured by homodyne measurement. Here, although the photon interacts with a number of qubits, it is usually released to the output. The detection efficiencies and SNR ratios change with the temporal profile of the incoming photon, such as Gaussian, decaying exponential, and rising exponential.

A more simple experimentally feasible QND photon detection method[9] uses a dispersive readout of a transmon in a far detuned cavity. A 1D transmission line as an input pulse mode. It then gets entangled with the transmon qubit after interacting(reflecting) with it. The qubit cavity interaction in the system is given by $a^\dagger a \sigma_z$ where $a^\dagger$ and a are the creation and annihilation operators of the cavity and σ_z is Pauli Z operator of the qubit. The qubit state is controlled with a Rabi pulse i.e., the resetting of the qubit to the ground state. The qubit readout is done through dispersive readout by measuring the dispersive shift of 2χ at cavity frequency. Heterodyne detection is used to measure the quadrature, which gives a measurement of the readout pulse reflected by the cavity. The external coupling rate of the cavity is tuned equal to the dispersive shift. This allows the phase difference of the reflected field(to initial field) at cavity frequency to be approximately equal to π. Apart from the phase shift of the reflected field, reflectance and phase shift difference can also be observed as a measure of dispersive shift for qubit readout (**See Fig 3.3**). To realize such an experiment and understand the process physically, we look at the circuit diagram of the protocol (**See Fig 3.4**). The π phase shift acquired by the input pulse mode is dependent
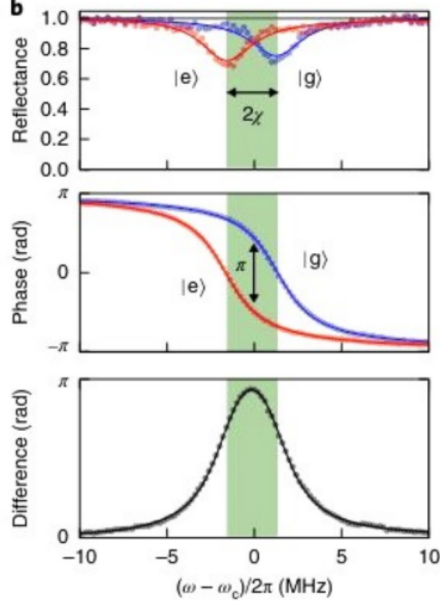
Figure 3.3: Reflectance (upper) , phase shift (middle) of reflected field and difference in phase shift plotted as a function of the probe field frequency, with qubit being in the ground state (blue) or the excited state (red) (Adapted from ref. [9])
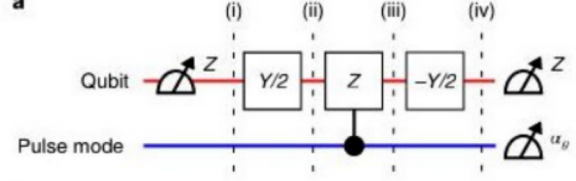

Figure 3.4: Circuit diagram of the proposal (Adapted from ref. [9])

on the qubit state so that it can be correlated with a controlled Z gate between the qubit and the input pulse mode. We see input mode as a superposition of single photon and no photon state with unequal probabilities, which signifies both the presence and absence of photon in the incoming field. Now the qubit state is supposed to be in superposition state when interacting with the incoming photon for it to entangle with it. In the circuit, a Ramsey pulse can be seen with a circuit initiated by Y/2, followed by a controlled Z gate and finally -Y/2 for measurement. The final state of the system after interacting(entangled) is $\sqrt{p_0}\,|g\rangle\,|0\rangle + \sqrt{p_1}\,|e\rangle\,|1\rangle$ where $|g\rangle$ and $|e\rangle$ are ground and excited state of the qubit and $|0\rangle$ and $|1\rangle$ are the 0 and single photon states of the incoming photon with probabilities p_0 & p_1 respectively. The fidelity of such protocol is observed to be around 0.84[9]. The dispersive shift observed can be around 2 MHz with a cavity decay rate of 0.30 MHz. T1 relaxation time is observed to be around $30\mu s$ and T2 dephasing time of about $25\mu s$. Such a detection process has better efficiency and yet simple to implement experimentally.

16

Indirect detection has an advantage over Direct detection that the incoming photon is not lost. Although it may seem a trivial thing, it has enormous implications on the behavior and applications of the detector. Along with preserving the incoming photon, QND detection allows detecting photon in a continuous manner. Such detectors were initially proposed for the detection of gravitational waves[] to overcome the effect of backaction on the measurement system. QND detections also play a crucial role in the fields of quantum error correction, quantum communication, and quantum computers. Although QND detection is more useful than direct detection and has a lot of applications, there are some challenges. One major challenge is because of the continuous measurement of the qubit state. The continuous measurement causes backaction, which affects the efficiency of the detector. Quantum Zeno effect states that, when a system which is observed to have random quantum jumps does not change it's state or appears to be frozen when the system is being observed continuously. The quantum Zeno effect caused by this backaction affects the detector fidelity[15]. This results in many photons remaining undetected. Such a challenge is hard to overcome and can be overcome by controlling the time for which the qubit state is being observed by looking at the qubit in some definite time intervals. We now have discussed what the previous approaches have been applied for building a photon detector. We will look at how we modeled and designed our detector qubit and the results in the following sections.

Chapter 4

Modelling the Detector

Now that we have seen the existing methods and their approaches to a superconducting photon detector, we turn to our method. However, before designing the detector, the detector should have a mathematical model to know what we should expect when we run the experiment. We initially look at the qubit-cavity system with a given hamiltonian and study cavity responses concerning the qubit state. We follow it by simulating quantum jumps, and it's response in the cavity. The reason to study this is that we want to ensure how plausible the qubit readout is when coupled to the cavity and other factors. Followed by that, we study the emitter-absorber system i.e. qubit-qubit-cavity system, where one qubit acts as an emitter while the other acts as an absorber with absorber being coupled to a cavity. This system acts as a near-perfect depiction of a microwave photon detector where the emitter and absorber are on the same chip with the absorber coupled to the cavity. Finally, we simulate the above systems to maximize the cavity's response for qubit readout by changing different parameters such as the power of the cavity(cavity photon number), drive strength.

4.0.1 Setting up the Hamiltonian

The general hamiltonian we use for a qubit-cavity system is $\sigma_x \sigma_x$ coupling interaction. The complete hamiltonian is as follows :

$$H = (\omega_q - \omega_d)a_q^\dagger a_q + (\omega_c - \omega_d)a_c^\dagger a_c + g(a_q a_c^\dagger + a_q^\dagger a_c) + \omega_d X_c$$

The first two terms are harmonic oscillator representation of qubit and cavity respectively. The third term indicates the qubit-cavity interaction in presence of RWA approximation

with g as coupling constant. A signature of strong coupling is the splitting of the cavity transmission peak into a pair of resolvable peaks when a single resonant atom is placed inside the cavity : an effect known as vacuum Rabi splitting. The terms $a_q a_c$ and $a_q^\dagger a_c^\dagger$ violate energy conservation. The former de-excites the atom and simultaneously absorbs a photon, and the latter excites the atom while it emits a photon. By contrast, the two terms we have kept conserve energy. The fourth term is the cavity being driven continously where $X_c = a_c + a_c^\dagger$ The hamiltonian is rotating frame wrt drive frequency ω_d. We set the qubit frequency at about 4.1 GHz and the cavity at 7.3 GHz and the cavity is being driven at the same frequency. The coupling is varied from 100-200 MHz. The cavity has a decay rate of about 31 MHz. When another qubit is added, the qubit-qubit interaction is sigma XX interaction.

We want to initiate by defining what the qubit ground and excited state are in terms of our observables. In a qubit-cavity system mentioned above, we start by measuring X, Y & Z expectation values of the qubit when the qubit is in ground state and when it's in excited state.

The X, Y & Z expectation values are $a_c + a_c^\dagger$, $-\iota(a_c - a_c^\dagger)$ & $a_c^\dagger a_c$(photon number) respectively. We can see that the X_c changes the sign and converges at different points for ground and excited states. However the Y_c & Z_c remains the same. As the annihilation operator a is of the form of $\hat{x} + \iota\hat{p}$ and the creation operator $a^\dagger$ is $\hat{x} - \iota\hat{p}$, the expectation value X_c i.e. $a_c + a_c^\dagger$ corresponds to position expectation value and Y_c i.e. $-\iota(a_c - a_c^\dagger)$ corresponds to momentum expectation value. Now as we change the position of qubit from 0 to 1 in hilbert space, we get a sign change in expectation value of X_c, however the momentum remains the same and hence we have no change in the Y_c expectation value as we change the qubit state. As the cavity has a decay rate of 31 MHz, we expect a decay of photons(Z_c expectation value is number of photons in cavity) into the environment.

The general state of a qubit according to quantum mechanics can be a coherent superposition of both 0 and 1. Unlile it's classical counterpart where measuring the bit doesn't affect the bit, measuring a qubit disturbs the superposition. When a qubit is measured, the superposition state collapses to a basis state, here either 0 or 1. As we have established a qubit-cavity system, we want to check cavity's response to the collapse of qubit superposition state. We here observe the cavity's response by heterodyne measurement i.e we plot X_c & Y_c with time. The graph was plotted by measuring for three instances; the qubit state being in 0, 1 and superposition state. We can observe the X quadrature for ground state(blue), excited state(orange) and superposition state(green). The collapse can be seen clearly. The

plot shows the heterodyne measurement for two different runs where we can see that the qubit state can collapse in either 0 or 1 (See Fig. 4.1).

However when we look at Y_c i.e Y quadrature we can see that there's very little information
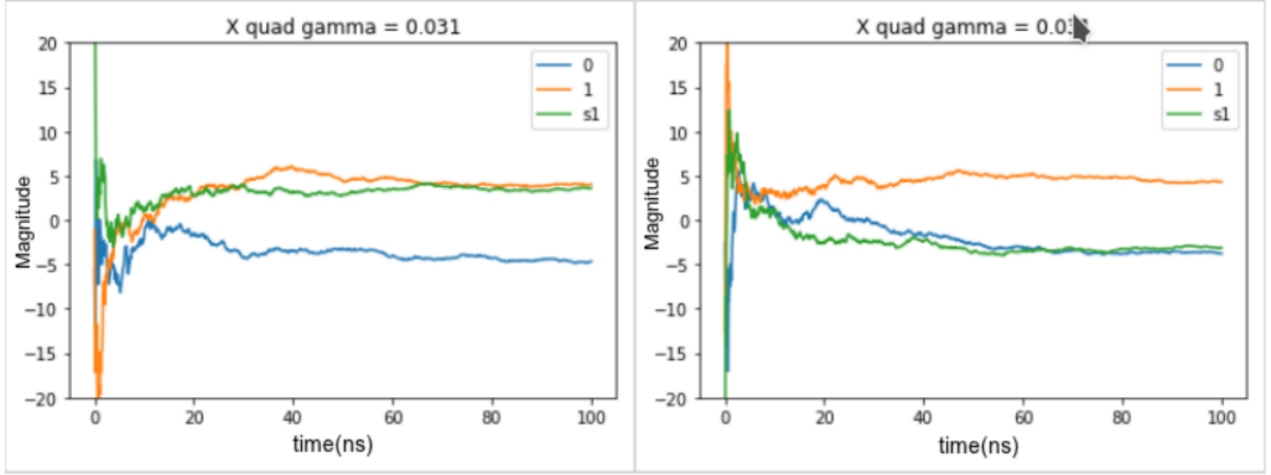

Figure 4.1: Heterodyne X quadrature

about the qubit state as we don't see much difference in all three qubit states (See Fig. 4.2). To avoid this issue and get maximum possible information about the qubit state, we instead use homodyne detection. Homodyne detection, a simplification of Heterodyne detection, where the local oscillator frequency equal to signal frequency. In Homodyne detection, we only have X quadrature(X_c) as an observable. Fig 4.3 and 4.4, indicate two different runs where the qubit was in superposition state and the collapse in ground or excited state is observed. To get a larger perspective of the qubit state collapse, we plot the Homodyne measurement for 30 individual runs and overlap them in **Fig 4.5**. We can see the qubit state collapsing in either ground state or excited state.

Now that we have calibrated our qubit-cavity system it's time to move on to Quantum jumps. We know that if qubit is in superposition state it will collapse onto it's basis states, but we don't have information about evolution of the qubit state when it collapses. We want to observe the collapse and also modify the system by adding another qubit and checking the cavity response then.

4.0.2 Quantum Jumps

Quantum trajectories can be described as a form of quantum measurement theory of continuous observation of a damped quantum system. Generally, it's used to describe open

21
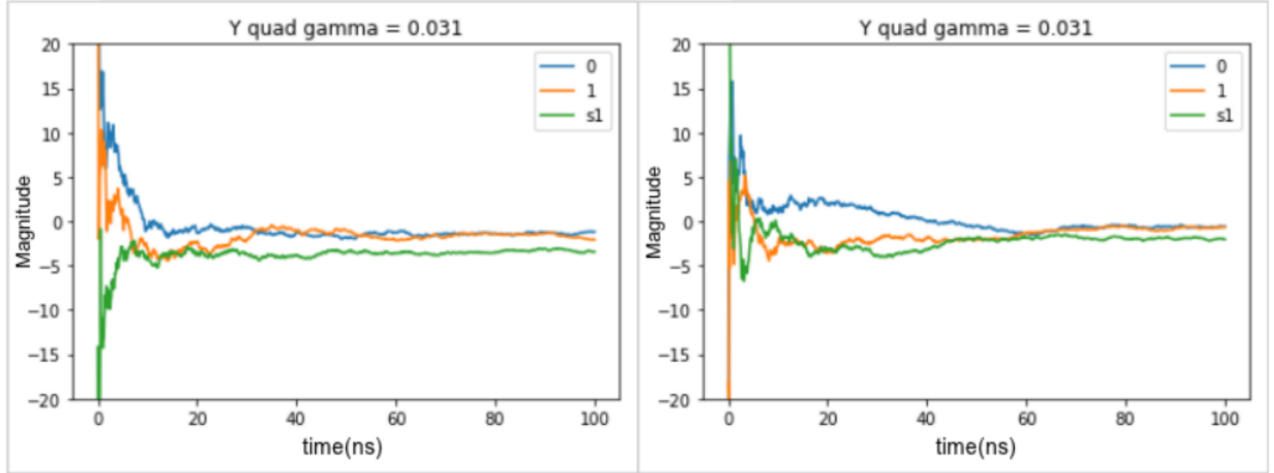
Figure 4.2: Heterodyne Y quadrature
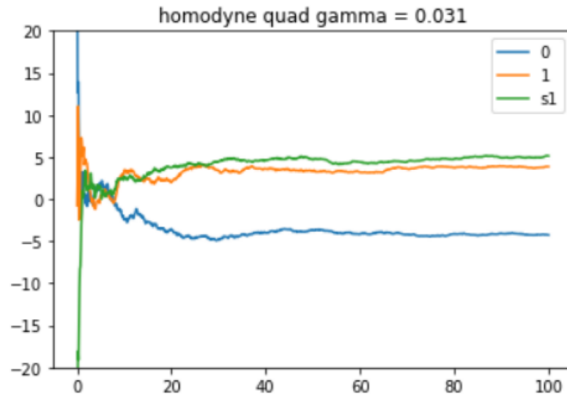
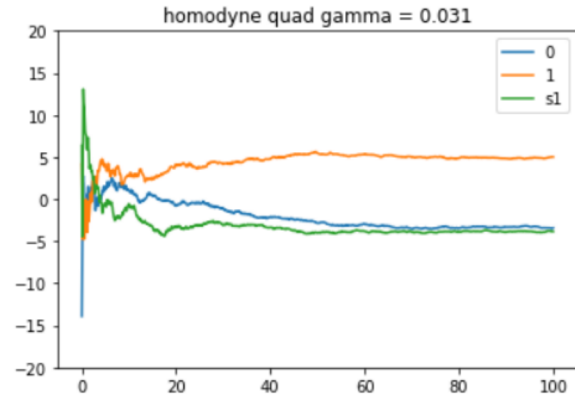Figure 4.3: Homodyne X quadrature:run 1   Figure 4.4: Homodyne X quadrature:run 2

quantum systems, which are measured continuously through time. Many groups have managed to control the quantum jump once it had started by applying an electric pulse to the artificial atom, in our case, a transmon. The quantum jumps are not truly instantaneous and can be observed in a controlled environment.

Now to efficiently detect a microwave photon, qubit readout is essential. Whenever the qubit absorbs a photon and gets excited, we should be able to know this in a continuous fashion to maintain them, it's nondemolition nature intact. Previously, we saw that the collapse of the qubit could be observed through the cavity's response given the cavity has a certain number of photons. Nevertheless, we do not yet know how the qubit will behave in the meantime. Here we will see the qubit state evolution and will compare it with the cavity's response. Now to observe the qubit state with time, we will use the density matrix of the entire system

22
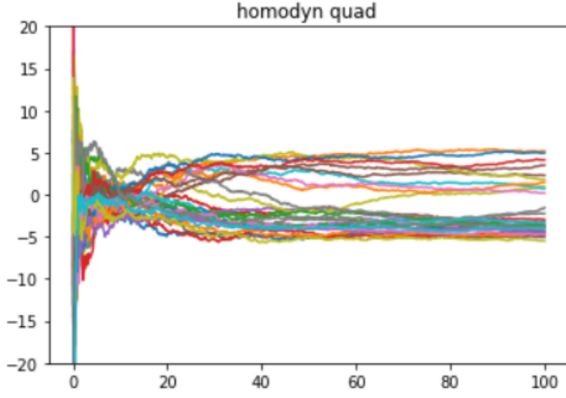
Figure 4.5: Homodyne X quadrature : Overlap of 30 individual runs

to extract the qubit's density matrix where the qubit state is stored at every time.

$$\rho = \rho_{qubit} \otimes \rho_{cavity}$$

where ρ is final density matrix of the qubit cavity system while ρ_{qubit} and rho_{cavity} are the density matrices of the qubit(2x2) and cavity(15x15) system. Now to find the qubit state at each point of time, we need density matrix of the qubit at each point of time. For this we take partial trace of the final density matrix, tracing out the cavity part.

$$\rho_{qubit} = Tr_1[\rho]$$

This gives us density matrix of a qubit at a particular point in time. Now for qubit in ground state(0 state) i.e $\begin{pmatrix} 1 \\ 0 \end{pmatrix}$ the density matrix is $\begin{pmatrix} 1 & 0 \\ 0 & 0 \end{pmatrix}$ and for qubit in excited state(1 state) i.e $\begin{pmatrix} 0 \\ 1 \end{pmatrix}$ the density matrix is $\begin{pmatrix} 0 & 0 \\ 0 & 1 \end{pmatrix}$. We can see the element A_{11} gives us an estimate of the state of the qubit given A is the qubit density matrix at a point in time. We plot the element A_{11} (qubit state) and it's conjugate A_{00} to observe the evolution of qubit state with time, given that $A = \rho_{qubit}$ at each point in time. The plots (**Fig 4.6, 4.7, 4.8, 4.9**) indicate the qubit state evolution along with the cavity's response when the qubit is in superposition state. The element A_{11} collapsing to 1 shows the qubit being in excited state and collapsing to 0 shows the qubit being in ground state. We can observe that qubit and cavity response are corresponding to each other. Now that we have simulated qubit-cavity system, it's time
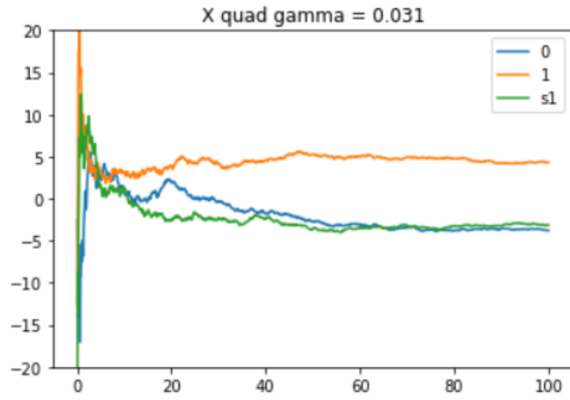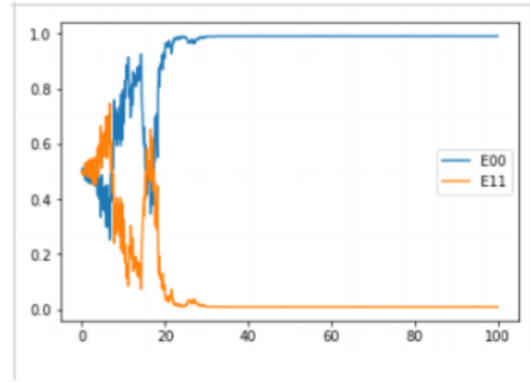
23

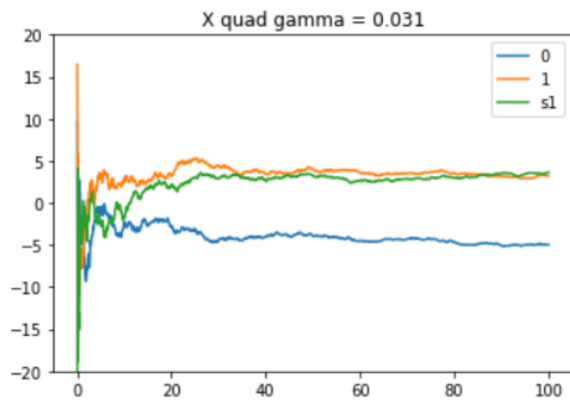Figure 4.6: Cavity Response

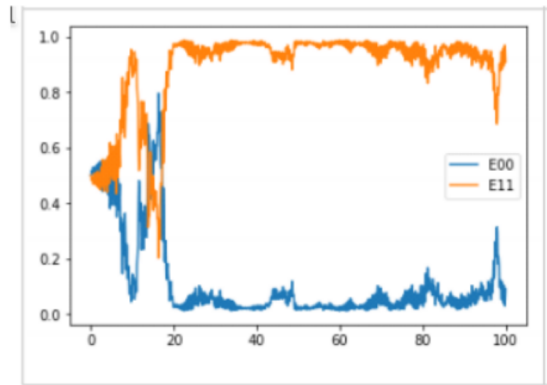Figure 4.7: Qubit state evolotion

Figure 4.8: Cavity Response

Figure 4.9: Qubit state evolution

to study the photon detector sytem. This will contain an extra qubit acting as an emitter and the existing qubit will act as absorber, with the absorber being coupled to the cavity. The emitter is initially in the excited state i.e contains a photon and the absorber in the ground state. When the qubit emits the photon spontaneously, the absorber qubit absorbs the photon and gets into excited state. We observe this absorber qubit via cavity's response to qubit's excitation. However this emittion is not a one transition process. The absorber after getting into excited state also emits photon which is then aborber by the emitter qubit. This oscillatory process goes on and is known as Vaccum Rabi oscillation (Fig 4.10). The frequency of these oscillation depends on coupling between emitter and absorber. Now in complex system as such, we have to make sure the qubit readout is perfect. This readout depends on various parameters such as qubit-cavity coupling, qubit-qubit coupling, cavity drive strength(cavity no. of photons). We here observe the absorber qubit's state evolution
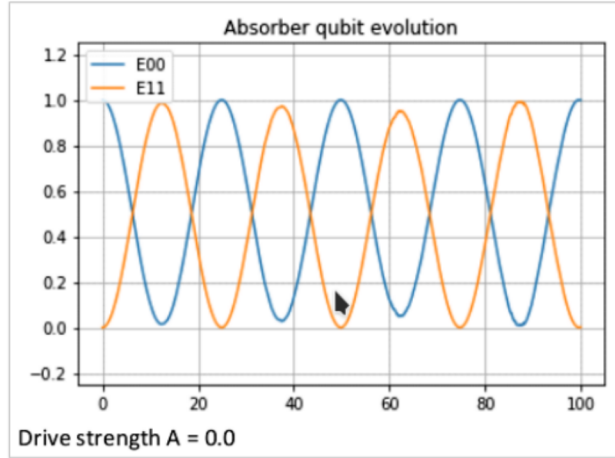
24

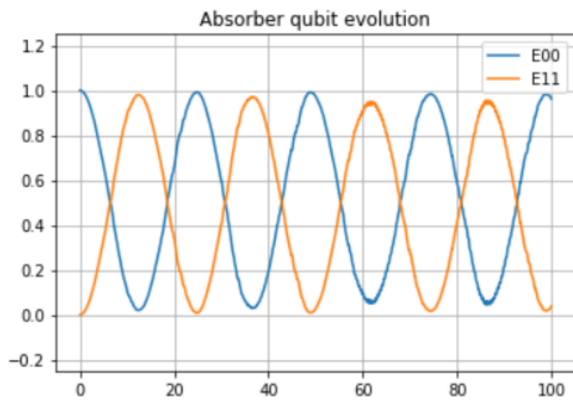Figure 4.10: Emitter-Absorber system : Rabi Oscillation

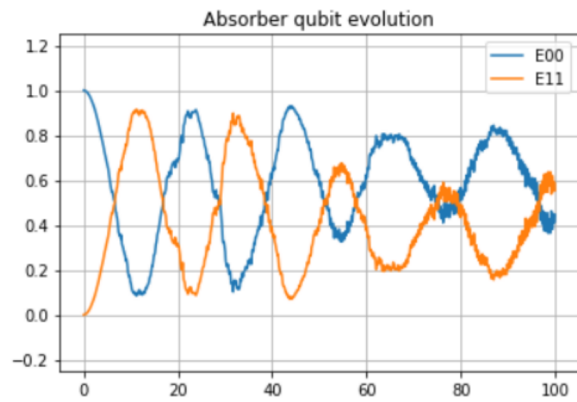

Figure 4.11: Emitter-Absorber system : A = 0.02

Figure 4.12: Emitter-Absorber system : A = 0.05

with time as we change the cavity drive strength to check how strongly can we measure the qubit state (Fig 4.11, 4.12, 4.13, 4.14). The qubit-qubit interaction here is basic σ_{XX} interaction with coupling constant of around 100-150 MHz. The qubit cavity interaction is same as above. The drive strength is varied from 20 MHz to 90 MHz.

Now that we have studied different systems and their effects upon varying different parameters of system. We have studied the homodyne detection and seen the cavity's response to the qubit's state evolution. We have also seen how the qubit behaves with number of photons in the cavity. Until now we have not used any physical model to simulate the qubit. In the next section we will simulate the qubit design depending on physical parameters such
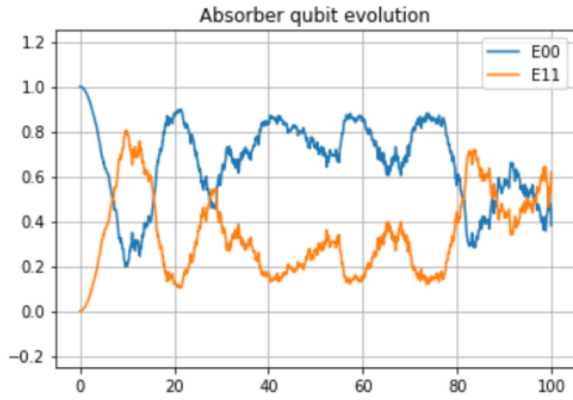
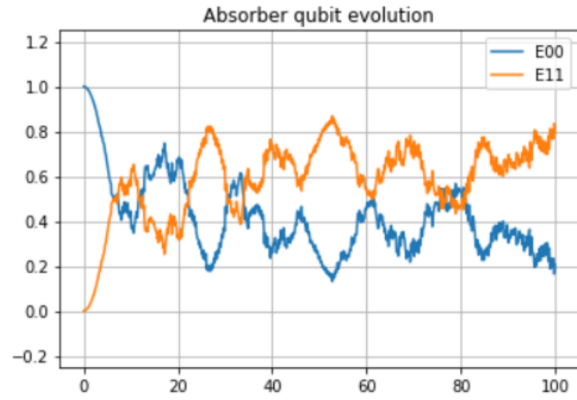25

Figure 4.13: Emitter-Absorber system : A = 0.07

Figure 4.14: Emitter-Absorber system : A = 0.09

as capacitance, inductance. We will also also take into account the shape and dimentions of capacitor pads used to build this device. We will simulate more experimental variables such relaxation times and S11 parameters. We will also finalize the physical design of our qubit system.

26

Chapter 5

Designing the Detector

As we've seen the simulations concerning the qubit readout and simulating a perfect qubit and a cavity in presense of their interactions, along with a photon detector system(emitter-absorber), we should now look at the experimental factors and parameters in the system. In the following section we'll be designing a physical model using circuit elements such as capacitance, nonlinear inductors using both circuit simulations and simulating a built device. After studying the circuit simulations, we'll study the simulate the physical model of the device . This will determine the dimensions and shape of the qubit. The capacitance and the inductance values determine the frequency modes of the qubit and the anharmonicity necessary for the experiment. As in the transmon regime, the anharmonicity is a small perturbation on the harmonic behavior, we have maximize the anharmonicity while keeping the qubit frequency modes in the desirable range. We here present a 4 qubit circuit design of the detector (**Fig 5.1**). The C_r capacitance is the coupling capacitance. C_{ji} and E_{ji} are the junction capacitance and the josephson energy of the ith qubit. The C_{ji} along with C_r, gives you energy of the capcitance Ec, which is then used for $\frac{Ej}{Ec}$ as a measure of anharmonicity.

Now that we've seen the model circuit design, we will look into the physical modelling of the system. As we know the capacitance values determine the qubit modes and anharmonicities, we have target capacitance values for which the anharmonicities are maximum and the qubit frequencies are in the desirable range and are distinguishable. We initially propose a design (**Fig 5.2, 5.3**) with and without CPW(Coplanar waveguide) structure. CPW structure is basically metallic strip separated by two narrow slits from an infinite ground plane. The capacitor pads are fabricated on a silicon chip. The dimention of the capacitor pads, the shape and distance between them determines the capacitance values between two
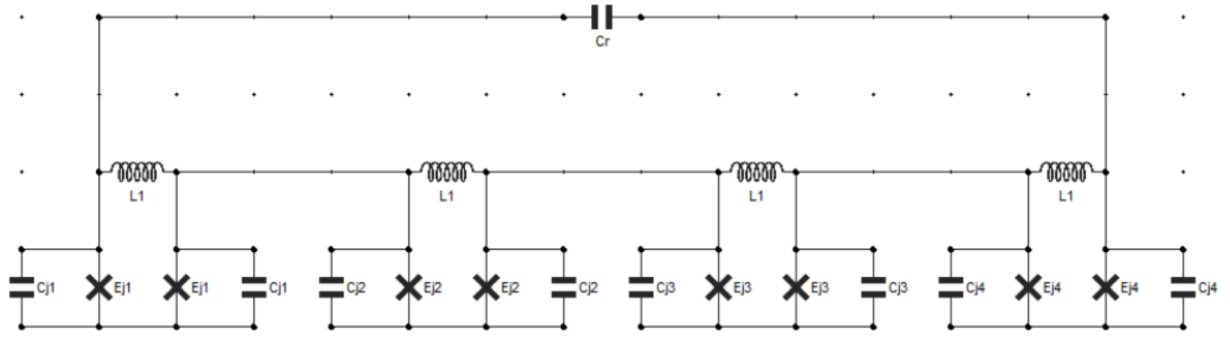
Figure 5.1: Proposed circuit diagram of 4-qubit system

pads. Between the two capacitor pads the qubit is fabricated.
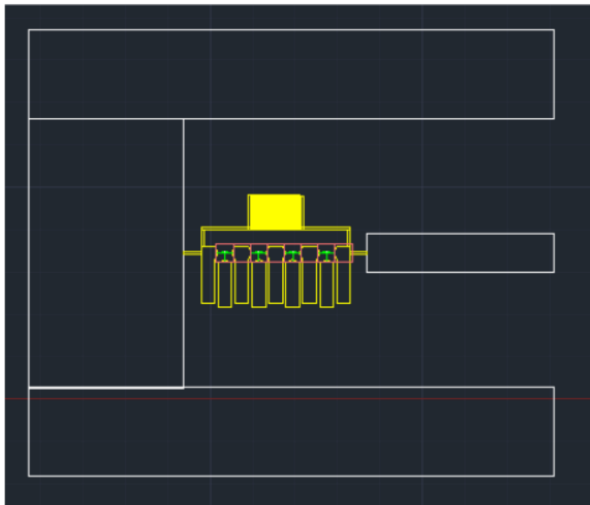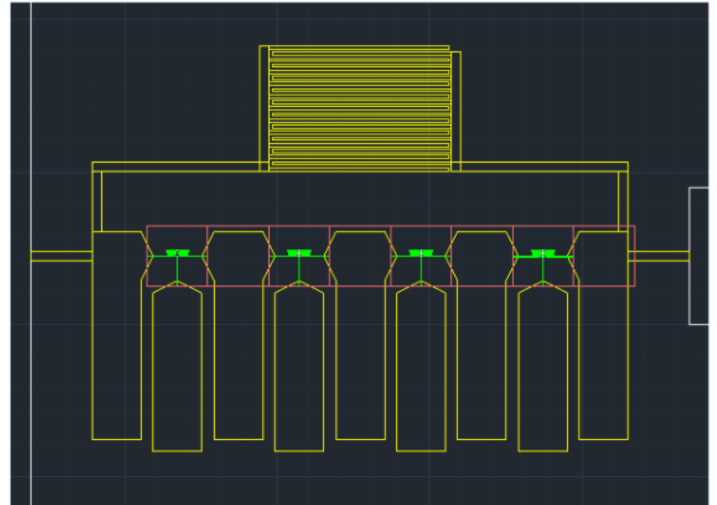

Figure 5.2: Proposed structure of the qubit

Figure 5.3

The initial proposed design is of course the basic design and modifications have to be done in order to get the right capacitance values. The design consists of 9 capacitor pads placed at an equal distance of 50um from each other. The length of each pad is around 300μm while the width is 80μm. These parameters obviously will alter as we try to change the cap values. We propose to get the capacitance values in the range of 30 to 40 fF(femto Farad)

with an interval of 2 fF. This should be such that C12 = C32, C43 = C54, C65 = C76 & C87 = C98 (where C_{ij} is capacitance between ith and jth capacitor pad). With the proposed capacitance values, we expect to see 4 qubit modes(4 frequencies) along with cavity frequency. The frequencies modes we expect to see are from 3.8 GHz to 4.8 GHz with intervals of 300 MHz. The anharmonicities are in the range of 200-250 MHz.

As we've seen the structure of the device, we'll see how the capacitance is calculated. So as C = Q/V, we need to set an overall voltage and then find the charge distribution to calculate the capacitance value. For every pad, we set the voltage of that pad to 1 and all others to 0. The charge distribution and the capacitance values are calculated in COMSOL. The electric potential of the design can be seen in **Fig 5.4**, where one of the pads has higher voltage and all others have lower.
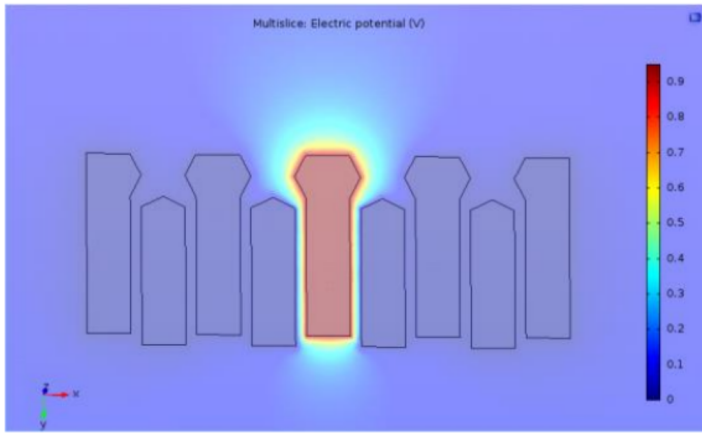

Figure 5.4: Electric Potential: 5th Capacitor pad has voltage 1V and others have 0V

To get the desired Cap values, the design is modified by changing the dimensions of the capacitor pads and making small cuts to the pads to finely tune the capacitance values. We are close enough with out targeted capacitance values. We get frequency modes of 4.02, 4.33, 4.57 & 4.84 GHz while all anharmonicities ranging from 220 MHz to 320 MHz. Notice that the qubit modes differ from each other by at least 240 MHz and anharmonicities are in the order of 220 MHz to 320 MHz. The capacitance values 31.1, 34.89, 37.29, 44.64 for C21, C43, C65 and C87 (which are equal to C32, C54, C76 & C98 respectively). As we've measured the capacitance values, we will move on to next part of circuit simulations.

29

After studying the simulations of the physical design, we want to take a look other exper-imental factors once the qubit is built. Decoherence is one of the most important parameter in deciding experiment's success. Coherence time T1 is the time for which the quantum superposition state survives without collapsing. Qubits always suffer from relaxation and dephasing, resulting in relatively short coherence times. Here we will study the how T1 varies with different set of parameters. **Fig 5.5** indicates a circuit diagram for single qubit coupled to a cavity. Here instead of nonlinear inductors, we use normal inductors as we are interested in plotting S11 with respect to freuqency. The values of the two qubit ca-pacitors(40.6 fF) are taken from the simulations ran above. The total cavity inductance is 400 nH . The qubit inductance is initially equal at 35 nH but varied as we'll see later. The external coupling capacitance is kept at 1 pF. The cavity is connected to a port of 50Ω via a coupling capacitance of 0.02401 pF.
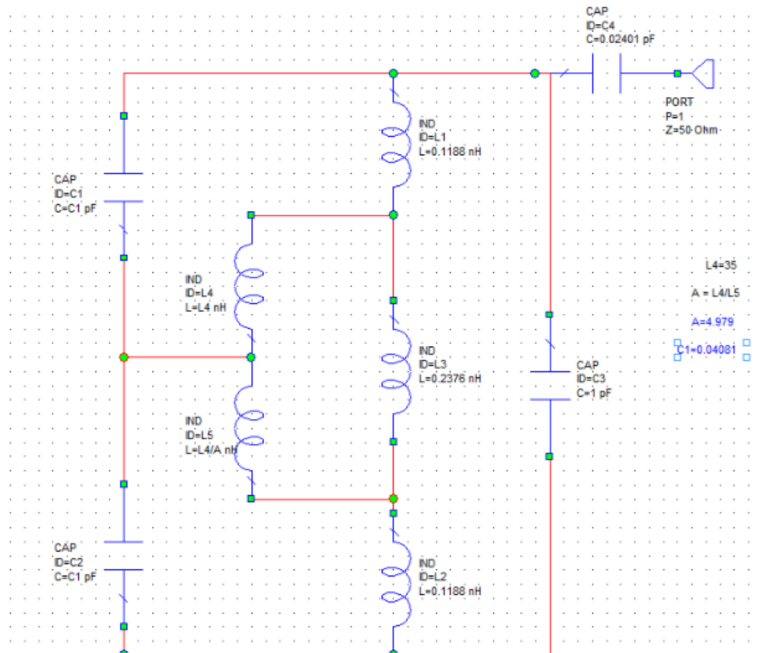

Figure 5.5: Single qubit circuit diagram

To study T1 we will be measuring the S parameters(S11) with respect to frequency(GHz). Here, the entire circuit acts as a black box and is connected to a port. The response of the system to the signal sent through the port are S parameters. The two parameters S11 and S12 are the reflective and the transmitive response of the input signal sent. So whenever the signal we're sending is of the resonant frequency, it won't be reflected and hence we expect a

dip in the S11 parameter. Here in **Fig 5.6**, we observe a regular plot of S11 parameter wrt frequency. We can see two dips in the curve indicating two modes, one of qubit and another of cavity. The parameters of circuit are changed so that the two plots are visible.

Now that we've seen S11, we can use it to calculate T1. In the circuit two qubit inductances,
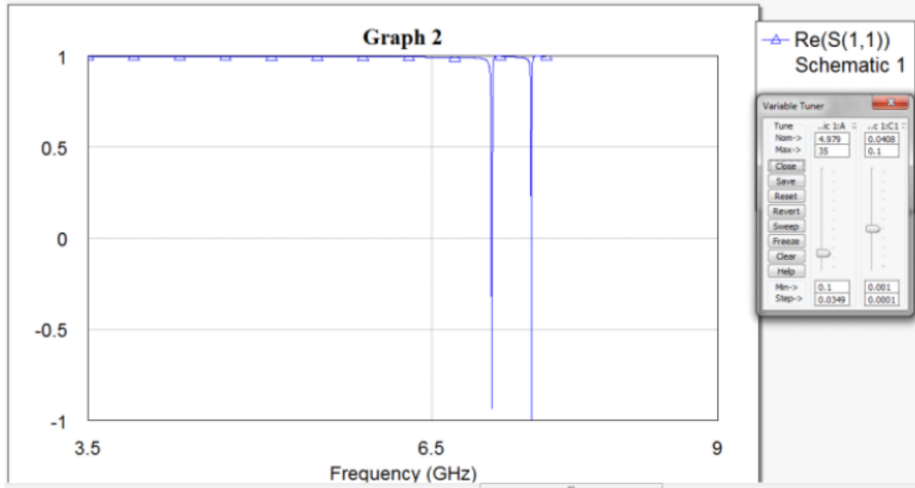

Figure 5.6: Varying S11 parameter with frequency

were initially equal. But when they're equal we don't expect to see a qubit mode in the S11 plot. So we need to slowly vary the difference between the inductances. We imagine the two inductors to be of the value L + β & L - β. We then plot T1 values with respect to β/L i.e the asymmtry in the inductances where L is 35 nH.

Now we can calculate T1 by two methods, one by avoided crossing method and another by measuring the linewidth. When the qubit resonant frequency is close enough to cavity resonant, we observe avoided crossing because of vaccum rabi splitting. Using this graph, we can find the coupling(g) as distance between the twoo peaks when they're just seperable. We know,

$$T1 = \frac{1}{\kappa}(\frac{\Delta}{g})^2$$

so given the coupling we can find T1. Another direct way is by looking at the linewidth of S11 peak at the qubit resonant frequency. T1 is just $1/\kappa$. We'll observe both these methods and see how the T1 varies with asymmetry in both the methods (**See Fig 5.7**). We observe that when we use the avoided crossing method we get much lower values of T1 when compared to the T1 values we get while calculating using linewidth. We find that using linewidth of the qubit resonant frequency gives much reliable values of T1 as it uses minimal variation in
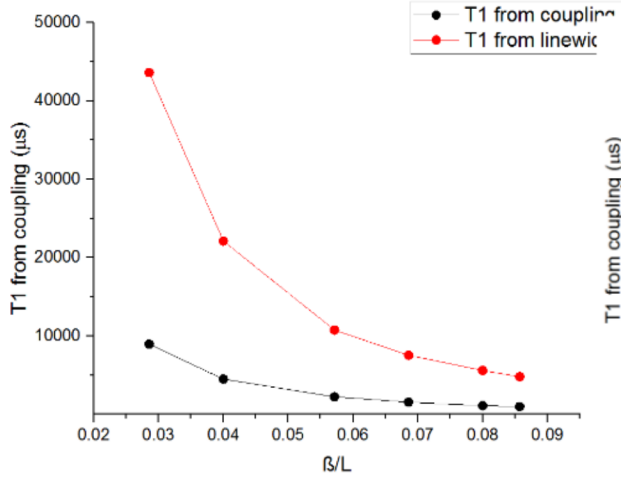
31
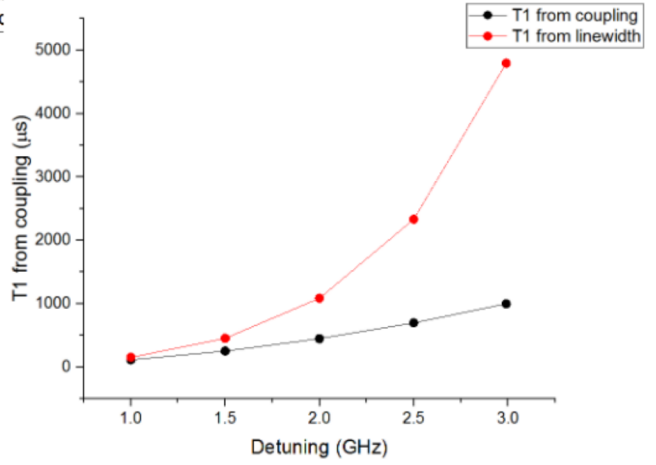
Figure 5.7: T1 variation with inductance asymmetry

Figure 5.8: T1 variation with detuning

the system parameters. Apart from coupling, another factor T1 depends on is detuning. We simulate T1 again by both methods and vary it with detuning (Fig 5.8). As the relaxation time depends on detuning with the relation $T1 \; \alpha \; (\delta)^2$, we get the expected behaviour. We can see the quadratic nature of the graph as expected.

We will look at the results and measurement procedures in the next section. We will discuss the experiments we performed to calculate the qubit resonant frequency and will talk about the coherence measurements made on the qubit design. We will discuss the drawbacks of our designs and also summarize the thesis.

Chapter 6

Results & Discussion

After simulating and predicting the behaviour of qubit and it's different properties and trends, we need to verify the results experimentally. We check the single qubit design and it's properties and discuss how experiment fits with our simulations. We also carry out Ramsey experiment to find out exact qubit frequency. In the latter part of the section, we will discuss the outcomes of this thesis, what are the trends in the result and their possible reason, and what could be done in future.

We initiate by measuring the qubit frequency as accurately as we can. In the dispersive approximation, the cavity resonant frequency depends on state of the qubit. Depending on the state of the qubit, the cavity frequency shifts by 2χ. The phase of the cavity photons can be used as a measurement for qubit state readout, using the interaction between qubit and cavity. We checked the reflected phase by passing the signal through one line and measuring the reflected phase through another line to avoid interference, after interacting with the qubit. To check what the qubit frequency is, need to sweep over a range of frequency to see what result we get. Now as we know, the reflected phase of the qubit in ground state, shifts by an amount of 2χ, at any particular frequency, the phase response for ground state is always higher than that for excited state. Now when sweep through the frequency range, at resonance frequency of the qubit, the qubit absorbs the signal and gets in excited state. Here the phase response is completely changed, and the value suddenly drops, to give us a dip in the measurement. From an experimental point of view, the process is called a two tone spectroscopy measurement. We send one tone for for frequency sweep and the second tone is sent at cavity frequency. We track the phase response of the transmission signal of the second tone. Once the first tone is at qubit frequency, the cavity's phase response changes and we see a dip in the transmission signal measurement.

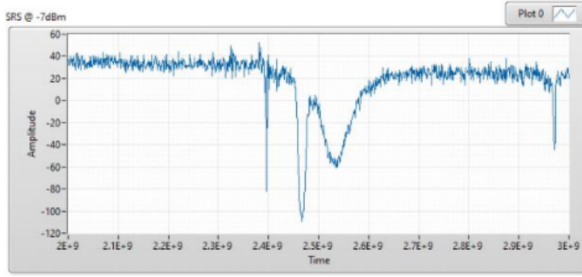Although ideally there should be only one transition based on the qubit resonant frequency,
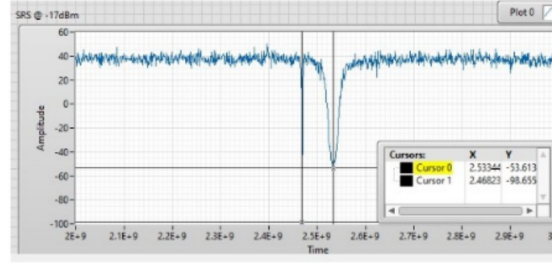

Figure 6.1: Power : -7 dbm

Figure 6.2: Power : -17 dbm

that is not the case. There are several other processes occuring depending on the power of incoming signal such as 2 photon processes. So although we get a dip in the measurement for $|0\rangle \longrightarrow |1\rangle$ transition, we also get a dip for $|0\rangle \longrightarrow |2\rangle$ via a two photon transition. The resonant frequencies of both the processes are close to each other. However, the higher photon transitions require high powered signal. We use this information to calculate the anharmonicity. The anharmonicity is given by ω_{10} - ω_{21}. We can also use alternative formula using ω_{10} - $\frac{\omega_{20}}{2}$ which can be derived easily. After finding the anharmonicity, the only thing to do is find the qubit frequency accurately. To achieve that, we lower the power of the incoming signal until we get a sharp peak at the qubit resonant frequency. We start with high power of -7 dbm(0.2 mW) and start decreasing the power. At around -17 dbm(20 μW), we can distinguish between two peaks, each for single photon transition and two photon transition. We calculate the anharmonicity which is the difference between two frequencies. We go on to reduce the power to see all the other peaks dissapear except one which we can now say is qubit frequency. At power approximately -47 dbm(20 nW) where we can clearly see a sharp peak for qubit resonance.

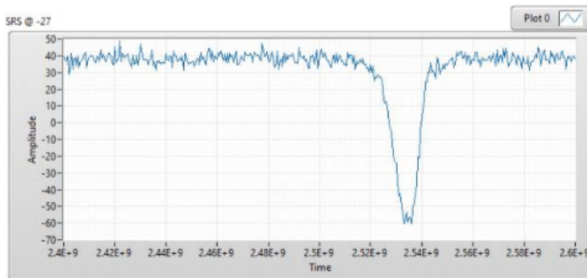The frequency is swept from 2 GHz to 3 GHz. We can see in the **Fig 6.1** the power is
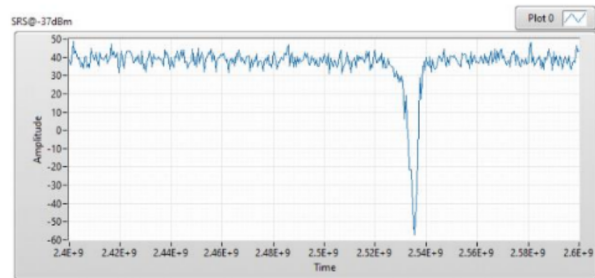

Figure 6.3: Power : -27 dbm

Figure 6.4: Power : -37 dbm

34

highest at -7 dbm and number of peaks are visible, for different transitions possible. **Fig 6.2** shows, at -17dbm only two peaks for two photon process transition and qubit resonant transition, to calculate anharmonicity. The anharmonicity turns out to be 65.21 MHz. In **Fig 6.3** we can see the all other peaks dissappear except the qubit transition. We can see the gradual narrowing of the width of the qubit frequency peak from **Fig 6.3 to 6.5**. The fig 3.5 shows a sharp peak at -47 dbm indicating it is the qubit resonant transition with a qubit frequency of 2.54 GHz.

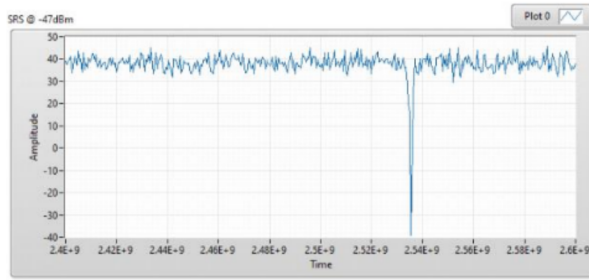Next we perform the coherence measurements on the qubit. To do that, we perform Rabi

Figure 6.5: Power : -47 dbm

experiment and relaxation time T1 measurements. We initiate by sending a microwave drive at ω_{01} frequency to see the Rabi oscillations (**see Fig 6.6**). We can see the qubit state oscillating from ground state to excited state. The time required for the qubit to change state from ground state to excited state or vice versa can be used to calibrate drive strength such that the π pulse length. We here observe the Rabi oscillation and calibrate the π pulse length to be 1815 ns. The relaxation time or 'longitudinal coherence time' T1 is the time requiured for the qubit to decay in ground state from excited state. T1 can be obtained by recording the evolution of the qubit after exciting the qubit by a π pulse. The measured evolution and the fit for exponential decay are shown in the Fig 6.7. The characteristic decay time T1 measured is 1.815 μs.

The qubit is prepared in a superposition state with a $\pi/2$ pulse, allowed to idle forsome timet, and then rotated back with another $\pi/2$ pulse and measured. The probability of measuring $|1\rangle$ varies sinusoidally in time, from 1 to 0, with the same frequency as the qubit. Ramsey experiment is also used to calculate the qubit frequency more accurately. The drive frequency to the experiment is detuned to the qubit frequency calculated from spectroscopy, by a small amount.This is most easily understood with the Bloch sphere representation: the initial $\pi/2$ pulse rotates the Bloch vector by $\pi/2$ about the X axis, and during the evolution it precesses at the qubit frequency about the Z axis. The final $\pi/2$ rotation about the X
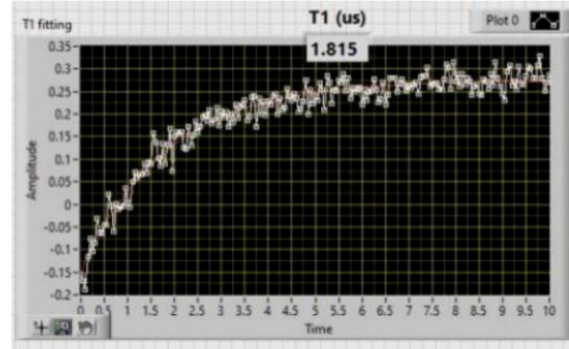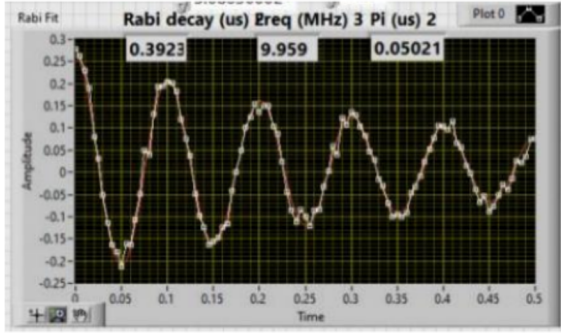
Figure 6.6: Vaccum Rabi Oscillations Experiment

Figure 6.7: T1 qubit state decaying from excited state to ground state

axis and measurement then projects the Y coordinate into the measurement basis. In the presence of dephasing, however, each iteration of the experiment will have a slightly different frequency. Therefore, the averaged Bloch vector is reduced in length, reducing the amplitude of the measured sinusoidal signal. For longer t, the spread is increased and the amplitude of the signal goes on decreasing (See Fig 6.8). The change in amplitude of the signal contains the information about the dephasing of the qubit.
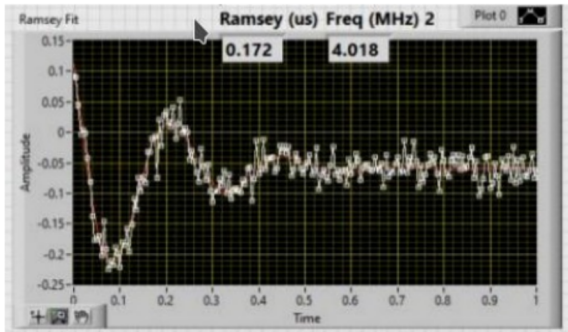

Figure 6.8: Ramsey Fringe experiment

From the Ramsey plot we can see that the decay is very rapid as the qubit lifetime is very low. Also the Rabi oscillations decay at higher decay rate. We tried using a CPW structure covering the qubit to increase the relaxation time but still got T1 time of $1.815\mu s$. Due to such low relaxation time, we could not proceed with the measurement of single photon detection. We initially started with 4 qubit system but reduced it to one qubit as in the four qubit system, four qubit modes were not distinguishable . We used the one qubit system to experimentally measure the T1 relaxation and T2 dephasing times. We carried out Ramsey fringe and Rabi oscillation experiment to study the dephasing and the decay of the qubit. A

two tone spectroscopy was carried out to calculate the qubit frequency and anharmonicity by lowering the power of incoming signal. For future work, extensive work must be done to increase the lifetime of the qubit. An on-chip single photon generator can be set up with long transmission line to make it itinerant. Work studied from the previous approaches (Ch. 2) can be beneficial in making the detector more efficient.

Bibliography

[1] G. Romero, J. J. Garca-Ripoll, and E. Solano. Microwave Photon Detector in Circuit QED. Phys. Rev. Lett. 102, 173602 (2009).

[2] Kono, S., Koshino, K., Tabuchi, Y. et al. Quantum non-demolition detection of an itinerant microwave photon. Nature Phys 14, 546549 (2018)

[3] Baptiste Royer, Arne L. Grimsmo, Alexandre Choquette-Poitevin, and Alexandre Blais. Itinerant Microwave Photon Detector. Phys. Rev. Lett. 120, 203602 (2018)

[4] B. Peropadre, G. Romero, G. Johansson, C. M. Wilson, E. Solano, and J. J. Garca-Ripoll. Approaching perfect microwave photodetection in circuit QED. Phys. Rev. A 84, 063834 (2011)

[5] Y.-F. Chen, D. Hover, S. Sendelbach, L. Maurer, S. T. Merkel, E. J. Pritchett, F. K. Wilhelm, and R. McDermott. Microwave Photon Counter Based on Josephson Junctions. Phys. Rev. Lett. 107, 217401 (2011)

[6] Inomata, K., Lin, Z., Koshino, K. et al. Single microwave-photon detector using an artificial Λ-type three-level system. Nat Commun 7, 12303 (2016)

[7] J. Wenner, Yi Yin, Yu Chen et al. Catching Time-Reversed Microwave Coherent State Photons with 99.4% Absorption Efficiency. Phys. Rev. Lett. 112, 210501 (2014)

[8] A. Narla, S. Shankar, M. Hatridge et al. Robust Concurrent Remote Entanglement Between Two Superconducting Qubits. Phys. Rev. X 6, 031036 (2016)

[9] S. R. Sathyamoorthy, L. Tornberg, A. F. Kockum, B. Q.Baragiola, J. Combes, C. M. Wilson, T. M. Stace, and G.Johansson. Quantum Nondemolition Detection of a Propagating Microwave Photon. Phys. Rev. Lett.112, 093601(2014)

[10] G. Oelsner, C.K. Andersen, M. Rehk et al. Detection of Weak Microwave Fields with an Underdamped Josephson Junction. Phys. Rev. Applied 7, 014012 (2017)

[11] R. H. Hadfield. Single-Photon Detectors for Optical Quantum Information Applications. Nat. Photonics 3, 696 (2009)

[12] X. Gu, A. F. Kockum, A. Miranowicz, Y.-X. Liu, and F.Nori. Microwave Photonics with Superconducting Quantum Circuits. Phys. Rep. 718, 1 (2017)

[13] Jean-Claude Besse, Simone Gasparinetti, Michele C. Collodo, Theo Walter, Philipp Kurpiers, Marek Pechal, Christopher Eichler, Andreas Wallraff. Single-Shot Quantum Nondemolition Detection of Individual Itinerant Microwave Photons. Phys. Rev. X 8, 021003 (2018)

[14] B. R. Johnson, M. D. Reed, A. A. Houck, D. I. Schuster,L. S. Bishop, E. Ginossar, J. M. Gambetta, L. DiCarlo, L.Frunzio, S. M. Girvin, and R. J. Schoelkopf. Quantum Non-demolition Detection of Single Microwave Photons in a Circuit. Nat. Phys. 6, 663 (2010)

[15] F. Helmer, M. Mariantoni, E. Solano, and F. Marquardt. Quantum nondemolition photon detection in circuit QED and the quantum Zeno effect. Phys. Rev. A 79, 052115 (2009)

[16] Schuster D., Circuit Quantum Electrodynamics, PhD dissertation, Yale University (2007)

[17] Slitcher D., Quantum Jumps and Measurement Backaction in a Superconducting Qubit, PhD dissertation, Yale University (2011)